# Thermal stress analyses of multilayered films on substrates and cantilever beams for micro sensors and actuators

INSTITUTE OF PHYSICS PUBLISHING JOURNAL OF MICROMECHANICS AND MICROENGINEERING

J. Micromech. Microeng. **16** (2006) 2509–2515 doi:10.1088/0960-1317/16/11/036

# Thermal stress analyses of multilayered films on substrates and cantilever beams for micro sensors and actuators

**C H Hsueh[1], C R Luttrell[1] and T Cui[2]**

[1] Materials Science and Technology Division, Oak Ridge National Laboratory, Oak Ridge, TN 37831, USA
[2] Department of Mechanical Engineering, University of Minnesota, Minneapolis, MN 55455, USA

E-mail: hsuehc@ornl.gov

Received 1 May 2006, in final form 27 July 2006
Published 10 October 2006
Online at stacks.iop.org/JMM/16/2509

**Abstract**
Thermal stress-induced damage in multilayered films formed on substrates and cantilever beams is a major reliability issue for the fabrication and application of micro sensors and actuators. Using closed-form predictive solutions for thermal stresses in multilayered systems, specific results are calculated for the thermal stresses in PZT/Pt/Ti/$SiO_2$/$Si_3N_4$/$SiO_2$ film layers on Si substrates and PZT/Pt/Ti/$SiO_2$ film layers on $Si_3N_4$ cantilever beams. When the thickness of the film layer is negligible compared to the substrate, thermal stresses in each film layer are controlled by the thermomechanical mismatch between the individual film layer and the substrate, and the modification of thermal stresses in each film layer by the presence of other film layers is insignificant. On the other hand, when the thickness of the film layer is not negligible compared to the cantilever beam, thermal stresses in each film layer can be controlled by adjusting the properties and thickness of each layer. The closed-form solutions provide guidelines for designing multilayered systems with improved reliability.

## 1. Introduction

During recent years, many efforts have been undertaken on the study of microelectromechanical systems (MEMS) based on piezoelectric thin-film materials and silicon technology, which include ultrasonic microsensors, force sensors for scanning force microscopy, accelerometers, cantilever actuators, ultrasonic micromotors and micropumps. The MEMS devices generally consist of multilayers of thin films on substrates or cantilever beams [1–5]. Lead zirconate titanate (PZT) thin film is one of the primary piezoelectric materials used in micro sensor or actuator applications. More attention has been attracted to the PZT film because its piezoelectric constants are much higher than other piezoelectric materials. Also, it can be deposited by various methods such as metal-organic chemical vapor deposition, sol-gel, metal organic decomposition, hydrothermal method, sputtering and pulsed laser deposition [6]. However, in the application of PZT films, thermal stresses have been identified as a problem which can induce cracking [7, 8] and affect operational functionality [9]. Because of the thermomechanical mismatch between constituent layers, the system is subjected to residual thermal stresses when it is cooled from the fabrication temperature or subjected to a temperature change during its applications. When the layer arrangement is asymmetric, the thermal stress distribution through the thickness of the system is also asymmetric which, in turn, results in bending. The curvature and the overall length change resulting from these thermal stresses have been measured [10].

Thermal stresses and bending in layered systems were first analyzed by Stoney in 1909 in which a bilayer strip consisting of a film and a substrate was considered, and a simple equation was derived to relate the stress in the film to the curvature of the system [11]. However, Stoney's equation is valid only when the film thickness is infinitesimal compared to the substrate thickness. The general solution for (elastic) thermal stresses in a bilayer system was first derived by Timoshenko in 1925 in which a bilayer strip subjected

  

to a temperature change was considered [12]. The analysis was based on classical beam theory and started by assuming the individual force and bending moment in each layer. The bending moment was related to the curvature of the layer, and both layers were assumed to have the same curvature. Then, by balancing the forces and moments in the system and by including the temperature-induced, the force-induced and the bending-induced strains to satisfy the strain continuity condition at the interface between the two layers, the solution was obtained. Timoshenko's approach has been adopted by many others to analyze the thermal stresses in multilayered systems [13–18]. However, for a multilayered system, both the number of unknowns to be solved and the number of continuity conditions to be satisfied at the interfaces increase with the number of layers in the system [13–18].

Recently, a simple analytical model for analyzing thermal stresses and deformation in multilayers has been developed, and the closed-form solutions are exact for locations remote from the free edges of the system [19, 20]. The essence of this model is to decompose the total strain through the thickness of the layered system into a uniform and a bending component, the continuity conditions at the interfaces are automatically satisfied and simple closed-form solutions for thermal stresses can be obtained by balancing forces and moments in the system. In this model, there are only three unknowns to be solved and three boundary conditions to be satisfied regardless of the number of layers in the system. While cracking in the PZT film layer resulting from thermal stresses is a major concern in its applications, the purpose of the present study is to apply the closed-form predictive solutions to systematically examine how the thermal stresses in the PZT layer can be controlled by varying the thickness of the constituent layer. First, the analytical model and the closed-form solutions for thermal stresses and deformation in multilayers are summarized. Second, results are calculated for the systems consisting of PZT/Pt/Ti/$SiO_2$ and PZT/Pt/Ti/$SiO_2$/$Si_3N_4$/$SiO_2$ film layers on Si substrates. In this case, the Si substrate is much thicker than the film layers, and the effects of introducing the intermediate film layers, $Si_3N_4/SiO_2$, between the $SiO_2$ film layer and the Si substrate are examined. Third, results are calculated for the systems consisting of PZT/Pt/Ti/$SiO_2$ film layers on $Si_3N_4$ cantilever beams. In this case, the thickness of film layers is not negligible compared to the thickness of the cantilever beam, and the effects of the thickness of each layer on the thermal stresses in PZT are examined. To validate the analytical results, the finite element analysis (FEA) is also performed.

## 2. Summary of the analytical model

The cross section of an elastic multilayered system is shown schematically in figure 1, where $n$ film layers with individual thicknesses, $t_i$, are bonded sequentially to a substrate with a thickness, $t_s$, at elevated temperatures. The subscript, $i$, denotes the layer number and ranges from 1 to $n$ with layer 1 being the one in direct contact with the substrate. Including the substrate, the system consists of $n$+1 layers. The coordinate system is defined such that the layer 1/substrate interface is located at $z = 0$, the free surfaces of the substrate and layer $n$ are located at $z = -t_s$ and $z = h_n$, respectively, and the

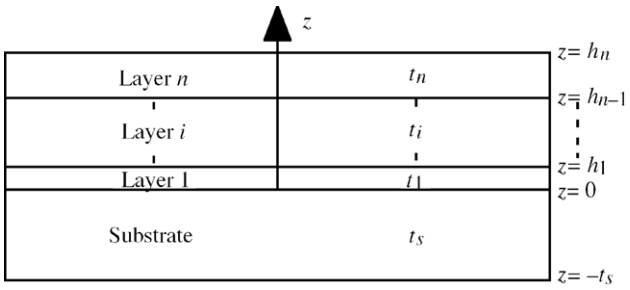


**Figure 1.** Schematic showing the cross section of multilayers and the coordinate system used in the analyses.

interface between layers $i$ and $i$+1 is located at $z = h_i$. With these definitions, the relation between $h_i$ and $t_i$ is described by

$$h_i = \sum_{j=1}^{i} t_j \quad (i = 1 \text{ to } n). \tag{1}$$

The multilayered system is subjected to a temperature change, $\Delta T$, and the coefficients of thermal expansion (CTEs) of the substrate and the films are $\alpha_s$ and $\alpha_i$, respectively. Because of the asymmetric layer arrangement, the thermal mismatch between layers results in the bending of the system. At positions away from the edges of the multilayered system, the stresses induced by the thermal mismatch are in-plane (i.e., parallel to the interface) and biaxial for the planar geometry, and both the stress normal to the interface and the interfacial shear stress are zero. By decomposing the total strain in the system into a uniform and a bending component, the in-plane biaxial stress distributions in the substrate and layers, $\sigma_s$ and $\sigma_i$, can be expressed as [19, 20]

$$\sigma_s = E_s' \left( c + \frac{z-b}{r} - \alpha_s \Delta T \right) \quad (\text{for } -t_s \leqslant z \leqslant 0), \tag{2a}$$

$$\sigma_i = E_i' \left( c + \frac{z-b}{r} - \alpha_i \Delta T \right) \quad (\text{for } i = 1 \text{ to } n), \tag{2b}$$

where $E' = E/(1-\nu)$ is the biaxial modulus, $E$ and $\nu$ are Young's modulus and Poisson's ratio, respectively, $c$ is the uniform strain component, $z = b$ denotes the position of the bending axis at which the bending strain component is zero and $r$ is the radius of curvature of the system.

The three parameters, $c$, $b$, and $r$, can be derived sequentially by satisfying the following three boundary conditions: (i) the resultant force due to the uniform strain component is zero, (ii) the resultant force due to the bending strain component is zero and (iii) the resultant bending moment due to the stresses described by equations (2*a*) and (2*b*) is zero. These three boundary conditions are described, respectively, by

$$E_s'(c - \alpha_s \Delta T)t_s + \sum_{i=1}^{n} E_i'(c - \alpha_i \Delta T)t_i = 0 \tag{3a}$$

$$\int_{-t_s}^{0} \frac{E_s'(z-b)}{r}\,\mathrm{d}z + \sum_{i=1}^{n} \int_{h_i-1}^{h_i} \frac{E_i'(z-b)}{r}\,\mathrm{d}z = 0 \tag{3b}$$

$$\int_{-t_s}^{0} \sigma_s z\,\mathrm{d}z + \sum_{i=1}^{n} \int_{h_i-1}^{h_i} \sigma_i z\,\mathrm{d}z = 0. \tag{3c}$$

**Table 1.** Elastic properties of the materials.

| Materials | $E$ (GPa) | $\nu$ |
|---|---|---|
| PZT | 75 | 0.31 |
| Pt | 170 | 0.39 |
| Ti | 110 | 0.34 |
| $SiO_2$ | 72 | 0.17 |
| $Si_3N_4$ | 222 | 0.28 |
| Si | 169 | 0.279 |

It should be noted that when $i = 1$, $h_{i-1}$ (i.e., $h_0$) is defined as zero.

With the above three boundary conditions, the solutions of the three parameters can be obtained, such that

$$c = \frac{\left(E'_s t_s \alpha_s + \sum_{i=1}^{n} E'_i t_i \alpha_i\right)\Delta T}{E'_s t_s + \sum_{i=1}^{n} E'_i t_i}, \tag{4a}$$

$$b = \frac{-E'_s t_s^2 + \sum_{i=1}^{n} E'_i t_i (2h_{i-1} + t_i)}{2\left(E'_s t_s + \sum_{i=1}^{n} E'_i t_i\right)}, \tag{4b}$$

$$\frac{1}{r} = \frac{3\left[E'_s(c-\alpha_s \Delta T)t_s^2 - \sum_{i=1}^{n} E'_i t_i (c-\alpha_i \Delta T)(2h_{i-1}+t_i)\right]}{E'_s t_s^2 (2t_s+3b) + \sum_{i=1}^{n} E'_i t_i \left[6h_{i-1}^2 + 6h_{i-1}t_i + 2t_i^2 - 3b(2h_{i-1}+t_i)\right]}. \tag{4c}$$

With the solutions of $c$, $b$ and $r$, the general solutions for the stress distributions in multilayered systems are complete. Both $\sigma_s$ in the substrate and $\sigma_i$ in each film layer given by equations (2*a*) and (2*b*) are functions of $z$. The above solutions are exact for positions in the multilayered system remote from the free edges, and the substrate and the films can have the comparable thicknesses. In the presence of the temperature dependence of CTE, the thermal strain $\alpha \Delta T$ should be replaced by an integral of the CTE with respect to the temperature. Alternatively, this thermal strain can also be expressed by $\alpha* \Delta T$ where $\alpha*$ is the average CTE within the temperature range. Also, the above solutions can be used to analyze the adsorption-induced deformation of multilayered sensors. In this case, the thermal strain, $\alpha \Delta T$, in the molecule recognition layer should be replaced by the adsorption-induced strain while the thermal strains in other layers are set to zero.

## 3. Results

Micro sensors and actuators based on PZT thin films have been batch fabricated by surface micromachining [6]. In this case, the PZT thin film is deposited on $Pt/Ti/SiO_2/Si$ substrates or $Pt/Ti/SiO_2/Si_3N_4$ cantilever beams and is then annealed at 700 °C in air to crystallize into the perovskite structure. This annealing process introduces thermal stress and bending in the system after cooling to room temperature. In the present study, $\Delta T = -680$ °C is used to calculate the biaxial thermal stresses in $PZT/Pt/Ti/SiO_2$ on Si wafers and $PZT/Pt/Ti/SiO_2$ on $Si_3N_4$ cantilever beams. The elastic properties of the constituent layer are listed in table 1 [7]. The CTEs vary with temperature and are listed in table 2 for the temperature ranging from 20 to 700 °C [7]. In order to validate the analytical solutions, the FEA is also performed. The multilayer is modeled using linear layered structural shell elements in the finite element code ANSYS, release 10.0, and the interfaces are assumed to remain bonded at all stages of computation.

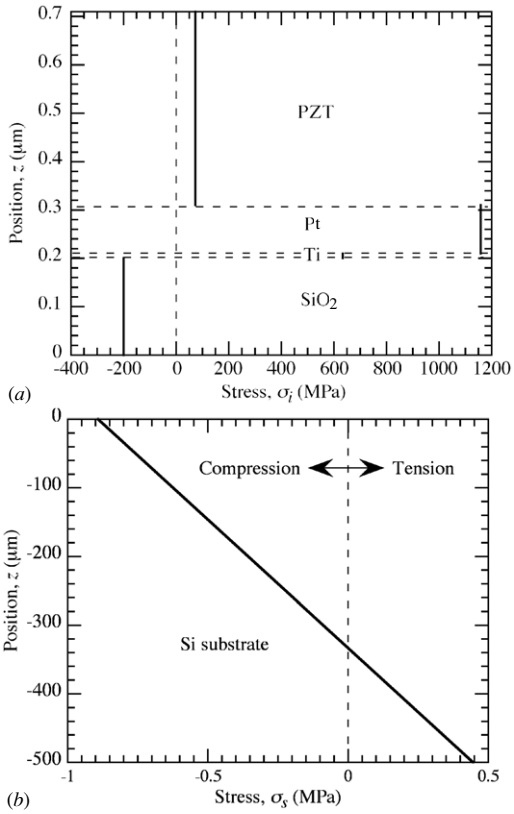


**Figure 2.** The biaxial thermal stress distribution through the thickness of (*a*) the film layers and (*b*) the substrate for $PZT/Pt/Ti/SiO_2$ film layers on the Si substrate.

**Table 2.** Coefficients of thermal expansion of the materials.

| Temperature T (°C) | Coefficient of thermal expansion, $\alpha$ ($\times 10^{-6}$ °C$^{-1}$) | | | | | |
|---|---|---|---|---|---|---|
| | PZT | Pt | Ti | $SiO_2$ | $Si_3N_4$ | Si |
| 20 | 1.8 | 8.92 | 8.74 | | | 2.616 |
| 200 | 1.0 | 9.5 | 9.1 | | | 3.614 |
| 300 | 0 | 9.7 | 9.28 | | | 3.842 |
| 350 | 6.2 | 9.96 | 9.37 | 2.25 | 0.4 | 3.929 |
| 400 | 7.8 | 10 | 9.4 | | | 4.016 |
| 500 | 8.2 | 10.2 | 9.7 | | | 4.151 |
| 700 | 8.2 | 11 | 9.98 | | | 4.26 |
| Average, $\alpha*$ | 4.775 | 9.9093 | 9.3868 | 2.25 | 0.4 | 3.788 |

The temperature dependence of CTE is considered in the FEA, and the interpolation scheme is performed in the FEA based on the input CTE data in table 2 to obtain the entire CTE versus temperature curve (for $T = 20$ to 700 °C). The total thermal strain for each material (i.e., the area under CTE versus the $T$ curve) is obtained from FEA. Dividing the total thermal strain by 680 °C, the average CTE, $\alpha*$, for $T = 20$–700 °C can be obtained for each material and is also listed in table 2 which is then used as the input for analytical modeling. Near the free edges, the simulated thermal stresses vary with the distance from the free edge. At locations sufficiently away from the free edges, the simulated thermal stresses become independent of the distance from the free edges and they are used to compare with the analytical results. The FEA results overlap with the analytical results in the present study, the analytical solutions

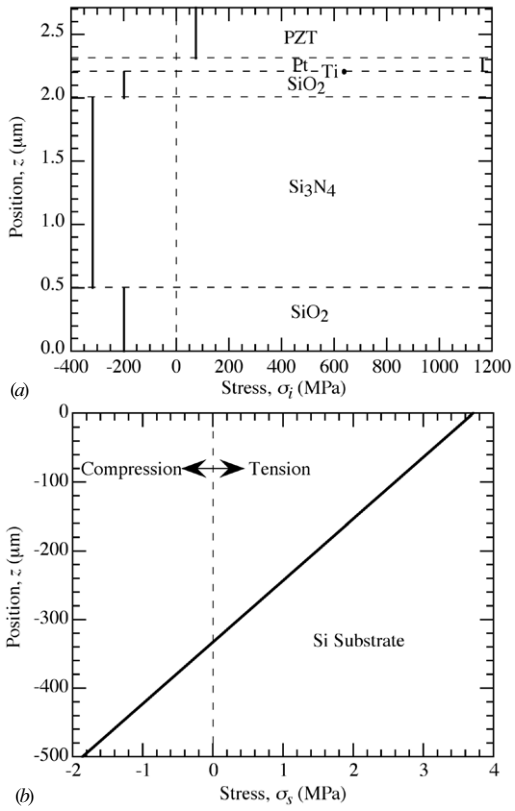


**Figure 3.** The biaxial thermal stress distribution through the thickness of (*a*) the film layers and (*b*) the substrate for $PZT/Pt/Ti/SiO_2/Si_3N_4/SiO_2$ film layers on the Si substrate.

given in section 2 are hence validated and only the analytical results are shown in the following.

### *3.1. Thermal stresses in PZT/Pt/Ti/SiO$_2$ film layers on Si substrates*

This system has been used for making acoustic emission sensors, and its fabrication process and the description of the functionality of each layer can be found elsewhere [8]. The layer thicknesses are: 0.4 $\mu$m PZT, 0.1 $\mu$m Pt, 0.01 $\mu$m Ti, 0.2 $\mu$m $SiO_2$ and 500 $\mu$m Si. In this case, the substrate is much thicker than the film layers. With the condition of $t_s \gg t_i$, the solutions given in section 2 can be simplified, such that

$$\sigma_s = \frac{2(3z+2t_s)}{t_s^2}\sum_{i=1}^{n} E_i' t_i(\alpha_i - \alpha_s)\Delta T \quad (\text{for } -t_s \leqslant z \leqslant 0 \text{ and } t_s \gg t_i), \tag{5a}$$

$$\sigma_i = E_i'(\alpha_s - \alpha_i)\Delta T \quad (\text{for } i = 1 \text{ to } n \text{ and } t_s \gg t_i). \tag{5b}$$

It can be seen from equation (5*a*) that the magnitude of thermal stresses in the substrate, $\sigma_s$, is relatively small because of $t_s \gg t_i$. Based on equation (5*b*), the variation of thermal stresses through the thickness of each film layer can be ignored (i.e., $\sigma_i$ is independent of $z$) when $t_s \gg t_i$. Also, the thermal stress in each thin film layer is controlled by the mismatch between the individual film layer and the substrate and is independent of the presence of other film layers. Stresses given by equations (5*a*) and (5*b*) are expressed in terms of the thermal

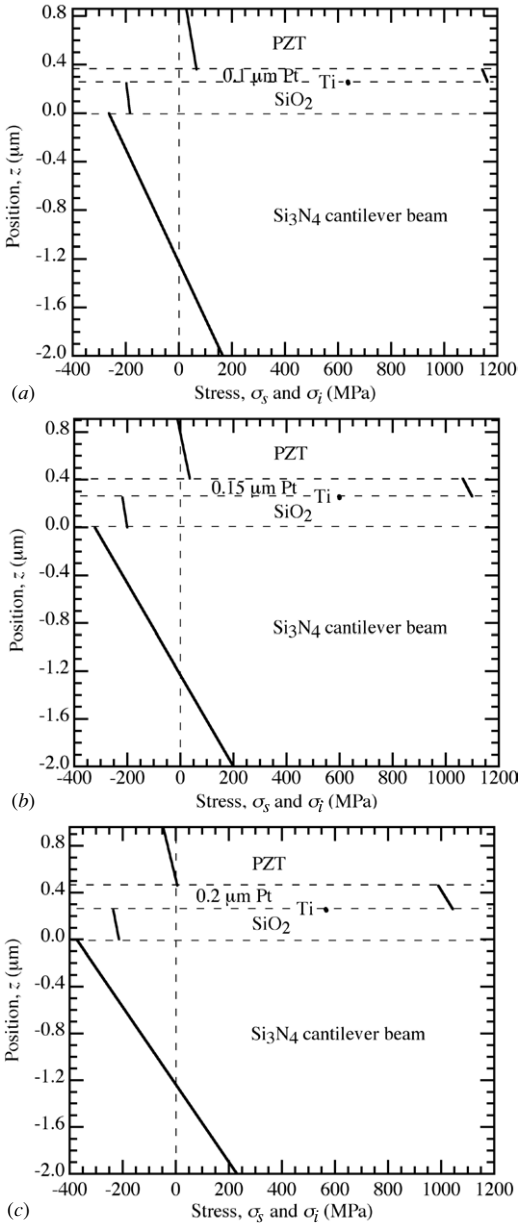


**Figure 4.** The biaxial thermal stress distribution through the thickness of $PZT/Pt/Ti/SiO_2$ film layers on the $Si_3N_4$ cantilever beam for Pt layer thickness of (*a*) 0.1 $\mu$m, (*b*) 0.15 $\mu$m and (*c*) 0.2 $\mu$m.

mismatch. Alternatively, these stresses can also be expressed in terms of the curvature, such that

$$\sigma_s = \frac{E_s'(3z+2t_s)}{3r} \quad (\text{for } -t_s \leqslant z \leqslant 0 \text{ and } t_s \gg t_i), \tag{6a}$$

$$\sigma_i = -\frac{E_s' t_s^2}{6t_i r_i} \quad (\text{for } i = 1 \text{ to } n \text{ and } t_s \gg t_i), \tag{6b}$$

where $1/r_i$ has the physical meaning of the component curvature contributed by the mismatch between the substrate and the individual film layer, such that

$$\frac{1}{r} = \sum_{i=1}^{n} \frac{1}{r_i} \quad (\text{for } t_s \gg t_i), \tag{7a}$$

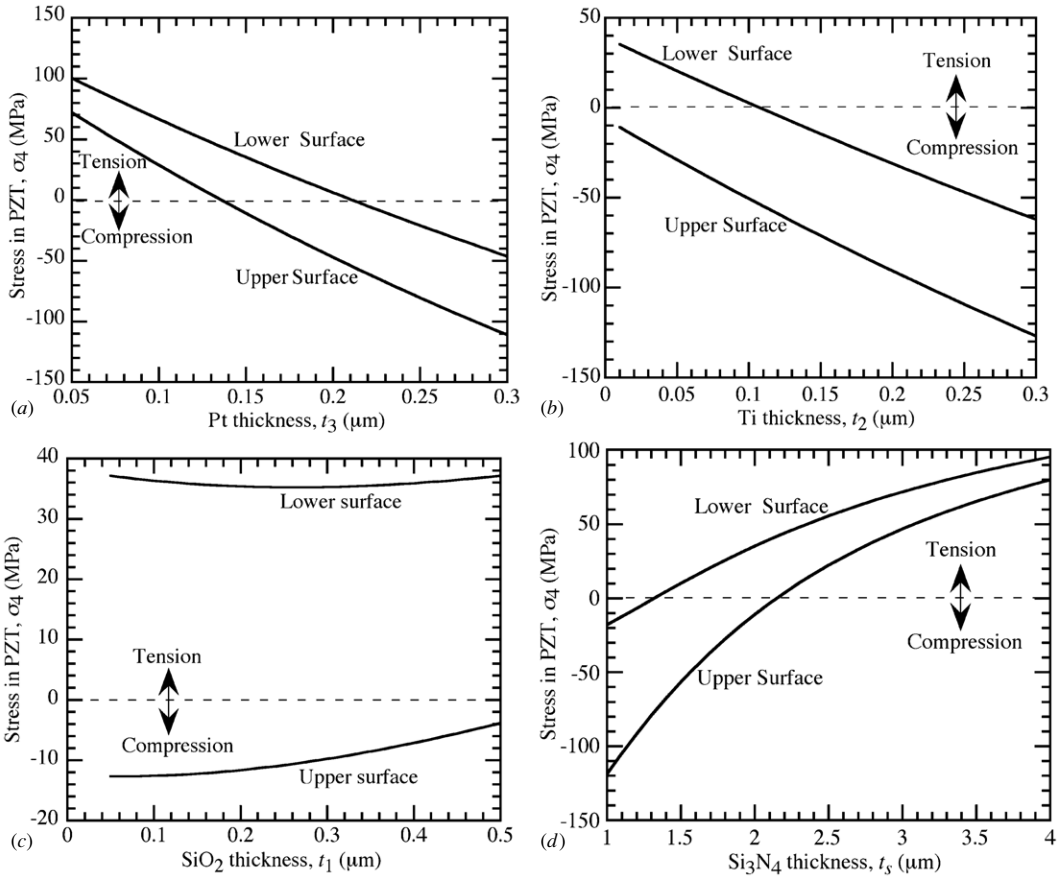


**Figure 5.** The effects of the thickness of (*a*) the Pt layer, (*b*) the Ti layer, (*c*) the $SiO_2$ layer and (*d*) the Si cantilever beam on the biaxial thermal stresses in the PZT layer for the system of PZT/Pt/Ti/$SiO_2$ film layers on the $Si_3N_4$ cantilever beam.

$$\frac{1}{r_i} = \frac{6E_i' t_i(\alpha_i - \alpha_s)\Delta T}{E_s' t_s^2} \quad (\text{for } t_s \gg t_i). \tag{7b}$$

Using the elastic properties listed in table 1 and the average CTE, $\alpha*$, listed in table 2, the thermal stresses (for $\Delta T = -680\,^{\circ}\text{C}$) through the thickness of the system calculated from equations (2) and (4) are shown in figures 2(*a*) and (*b*), respectively, for the film layers and the substrate. While the stresses in each film layer are almost uniform (figure 2(*a*)), the sign of stresses (i.e., tension or compression) depends on the comparison between $\alpha_s$ and $\alpha_i$. While the magnitude of stresses in the substrate is relatively small, the substrate is subjected to combined tension/compression because of the bending of the system (figure 2(*b*)). Also, the calculated curvature is $-0.114 \times 10^{-7}\ \mu\text{m}^{-1}$, and the concave surface faces up in figure 1.

The five-layered PZT/Pt/Ti/$SiO_2$/Si system has been used to fabricate the cantilever beam. This can be achieved by (i) adding 1.5 $\mu$m $Si_3N_4$/0.5 $\mu$m $SiO_2$ between the $SiO_2$ film layer and the Si substrate to form the seven-layered PZT/Pt/Ti/$SiO_2$/$Si_3N_4$/$SiO_2$/Si system, and (ii) etching (i.e., the released beam method). It is of interest to examine how the stresses shown in figure 2 are modified by adding two film layers in the system, and the results are shown in figures 3(*a*) and (*b*), respectively, for the film layers and the substrate. The calculated curvature is $0.475 \times 10^{-7}\ \mu\text{m}^{-1}$, and the concave surface faces down in figure 1. Compared to figures 2(*a*), 3(*a*) shows that stresses in the top four film layers, PZT, Pt, Ti and $SiO_2$, remain almost the same despite the presence of the two additional layers, $Si_3N_4$ and $SiO_2$. Compared to figure 2(*b*), figure 3(*b*) shows significant modifications of thermal stresses in the substrate because of the two additional layers. Also, while the Si substrate has a convex free surface for the five-layered system, it has a concave free surface for the seven-layered system. This is because the four film layers in the five-layered system have an effective CTE that is higher than the Si substrate. After adding $Si_3N_4$ and $SiO_2$ film layers which have lower CTEs compared to Si, the effective CTE of the six film layers in the seven-layered system become lower than the CTE of Si.

### *3.2. Thermal stresses in PZT/Pt/Ti/$SiO_2$ film layers on $Si_3N_4$ cantilever beams*

In this case, the cantilever beam is not much thicker than the film layers, and it is of interest to examine how the thermal stresses in the system are modified by the individual layer thickness. Unless noted otherwise, the following thicknesses are used in calculations: 0.5 $\mu$m PZT, 0.15 $\mu$m Pt, 0.01 $\mu$m Ti, 0.25 $\mu$m $SiO_2$ and 2 $\mu$m $Si_3N_4$. When the effects of the thickness of a specific layer are considered, its layer thickness is varied within a practical range while the thicknesses of other layers remain unchanged.

First, the effects of the thickness of the Pt layer are examined. The thermal stress through the thickness of the system is shown in figures 4(*a*), (*b*) and (*c*), respectively, for 0.1, 0.15 and 0.2 $\mu$m of the Pt layer. As the thickness of the Pt layer increases, the stresses in the other layers become more compressive or less tensile. This is because the Pt layer has the highest CTE among the five layers which, in turn, imposes compressive constraint on the other layers upon cooling shrinkage. The stress distribution is linear through the thickness of each layer. The curvature of the system shows that PZT is on the concave side and $Si_3N_4$ is on the convex side. As a result, the stress at the lower surface is always more tensile than the stress at the upper surface for the same layer. The present interest is to study how thermal stresses in the PZT layer change with the thicknesses of other layers. To illustrate this, the stresses at the upper and the lower surfaces of the PZT layer are plotted as functions of the Pt layer thickness $t_3$ in figures 5(*a*). When $t_3 < \sim 0.14$ $\mu$m, PZT is subjected to tension. When $\sim 0.14$ $\mu$m $< t_3 < \sim 0.21$ $\mu$m, PZT is subjected to combined tension/compression. When $t_3 > \sim 0.21$ $\mu$m, PZT is subjected to compression. The effects of thicknesses of Ti, $SiO_2$ and $Si_3N_4$ layers on the thermal stresses in PZT are shown in figure 5(*b*), (*c*) and (*d*), respectively. Compared to figures 5(*a*), (*b*) shows similar trend because both Pt and Ti have higher CTEs than PZT. On the other hand, figure 5(*d*) shows that the stresses in PZT become more tensile as the thickness of $Si_3N_4$ increases because $Si_3N_4$ has a lower CTE than PZT. Figure 5(*c*) shows that the effects of the $SiO_2$ layer thickness is relatively weak. This is because $SiO_2$ is softer than other layers, and the constraint imposed by the $SiO_2$ layer on other layers is weaker.

It should be noted that the calculated thermal stresses in the Pt layer are from 1000 to 1200 MPa (see figures 2, 3 and 4), which are well above the yield stress of Pt thin films. However, using the thermomechanical properties given in tables 1 and 2, the analytical results have been validated by FEA. The possible reasons for the high predicted stresses in the Pt layer are addressed as follows. The Pt layer is generally deposited by sputtering, and it forms a vertical columnar microstructure that works as a template for PZT to grow. Compared to bulk Pt, the Pt thin film would have lower in-plane modulus (i.e., more compliant) and CTE because of the columnar microstructure. While the thermomechanical properties of Pt cited in table 1 and 2 are for the bulk material, the thermal stresses in the Pt layer are expected to be over-predicted. Also, during the annealing process, atoms can migrate in the Ti and the $SiO_2$ layers which, in turn, result in stress relaxation. This stress relaxation is not considered in analytical modeling. In addition, the migration of Pt atoms at 500 °C has been reported [21]. In this case, if 500 °C is considered as the stress-free temperature and $\Delta T = -480$ °C is adopted in calculations, the predicted thermal stresses in the Pt layer become 700–850 MPa while the measured thermal stress of 550 MPa has been reported by Ledermann *et al* [10]. Finally, it should be noted that the oxidation of Ti could occur [22]. In this case, the thermomechanical properties of Ti should be replaced by those of $TiO_2$ in analyzing thermal stresses.

## 4. Conclusions

Thermomechanical mismatch between layers induces residual thermal stresses in the multilayered system. These stresses can result in cracking, affect the functionality of the film layer and create a major reliability problem for the applications of multilayered systems, e.g., micro sensor and actuators. Hence, it is crucial to be able to predict and control these stresses. The theoretical evaluation of these stresses often relies on finite element analyses to perform case-by-case studies. Recently, closed-form solutions for in-plane biaxial thermal stresses in multilayers have been derived, and the solutions are exact for locations away from the free edges of the system. These solutions are used in the present study to systematically examine the thermal stresses in multilayers of thin films formed on either thick substrates or thin cantilever beams. In the presence of a thick substrate, thermal stresses in each thin film layer are controlled by the mismatch between the individual film layer and the substrate and are insensitive to the presence of other film layers. Compared to the stresses in $PZT/Pt/Ti/SiO_2$ film layers formed on the Si substrate (figure 2), the stresses in $PZT/Pt/Ti/SiO_2/Si_3N_4/SiO_2$ film layers formed on the Si substrate (figure 3) show that and stresses in the top four layers, PZT, Pt, Ti and $SiO_2$, remain almost the same despite the presence of two additional layers while the two systems are curved in the opposite direction. With a thin cantilever beam as the structural support, the thickness of the film layer is not negligible compared to the cantilever beam, and thermal stresses in each film layer can be controlled by adjusting the properties and thickness of each layer. The closed-form predictive solutions provide guidelines for designing multilayered systems with improved reliability. Depending upon which layer is susceptible to damage in the multilayered system, the corresponding thermal stresses should be minimized by the judicious choice of layer properties/thicknesses guided by the closed-form solutions. Finally, it should be noted that although the analytical solutions are exact, the accuracy of the predicted stresses is contingent upon the determination of (i) the thermomechanical properties of each constituent layer and (ii) the temperature range for stress development. Also, when edge delamination is of concern, the subject can be found in a recent publication [23], which summarizes the existing work and develops a new approach in analyzing edge delamination of multilayers.

## Acknowledgments

The authors thank Drs P F Becher, P G Datsko and A Passian for reviewing the manuscript. This work was sponsored by US Department of Energy, Division of Materials Sciences and Engineering, Office of Basic Energy under contract DE-AC05-00OR22725 with UT-Battelle, LLC.

## References

[1] Lavrik N V, Sepaniak M J and Datskos P G 2004 Cantilever transducers as a platform for chemical and biological sensors *Rev. Sci. Instrum.* **75** 2229–53

[2] Wig A, Passian A, Arakawa E, Ferrell T L and Thundat T 2004 Optical thin-film interference effects in microcantilevers *J. Appl. Phys.* **95** 1162–5

[3] Dunning J, Fu X A, Rajgopal S, Mehregany M and Zorman C A 2004 Characterization of polycrystalline SiC thin films for MEMS applications using surface micromachined devices *Mater. Sci. Forum* **457–460** 1523–6
[4] Zinck C, Pinceau D, Defaÿ E, Delevoye E and Barbier D 2004 Development and characterization of membranes actuated by a PZT thin film for MEMS applications *Sensors Actuators* A **115** 483–9
[5] Mukhopadhyay R, Sumbayev V V, Lorentzen M, Kjems J, Andreasen P A and Besenbacher F 2005 Cantilever sensor for nanomechanical detection of specific protein conformations *Nano Lett.* **5** 2385–8
[6] Cui T, Markus D, Zurn S and Polla D 2004 Piezoelectric thin films formed by MOD on cantilever beams for micro sensors and actuators *Microsystem Technol.* **10** 137–41
[7] Zang M, Polla D, Zurn S and Cui T 1999 Stress and deformation of PZT thin film on silicon wafers due to thermal expansion *Mat. Res. Soc. Symp. Proc.* **574** 107–12
[8] Polcawich R G, Scanlon M, Pulskamp J, Clarkson J, Conrad J, Washington D, Piekarz R, Trolier-McKinstry S and Dubey M 2003 Design and fabrication of a lead zirconate titanate (PZT) thin film acoustic sensor *Integr. Ferroelectr.* **54** 595–606
[9] Muralt P 2000 Ferroelectric thin films for micro-sensors and actuators: a review *J. Micromech. Microeng.* **10** 136–46
[10] Ledermann N, Muralt P, Baborowski J, Forster M and Pellaux J P 2004 Piezoelectric Pb($Zr_x$, $Ti_{1-x}$)$O_3$ thin film cantilever and bridge acoustic sensors for miniaturized photoacoustic gas detectors *J. Micromech. Microeng.* **14** 1650–8
[11] Stoney G G 1909 The tension of metallic films deposited by electrolysis *Proc. R. Soc.* **82** 172–5
[12] Timoshenko S 1925 Analysis of bi-metal thermostats *J. Opt. Soc.* **11** 233–55
[13] Saul R H 1969 Effect of a $GaAs_xP_{1-x}$ transition zone on the perfection of GaP crystals grown by deposition onto GaAs substrates *J. Appl. Phys.* **40** 3273–9
[14] Olsen G H and Ettenberg M 1977 Calculated stresses in multilayered heteroepitaxial structures *J. Appl. Phys.* **48** 2543–7
[15] Feng Z C and Liu H D 1983 Generalized formula for curvature radius and layer stresses caused by thermal strain in semiconductor multilayer structures *J. Appl. Phys.* **54** 83–5
[16] Iancu O T, Munz D, Eigenman B, Scholtes B and Macherauch E 1990 Residual stress state of braze ceramic/metal compounds, determined by analytical methods and x-ray residual stress measurements *J. Am. Ceram. Soc.* **73** 1144–9
[17] Jou J H and Hsu L 1992 Bending-beam measurement of solvent diffusions in polyimides: theoretical and experimental *J. Appl. Polym. Sci.* **44** 191–8
[18] Liu H C and Murarka S P 1992 Elastic and viscoelastic analysis of stress in thin films *J. Appl. Phys.* **72** 3458–63
[19] Hsueh C H 2002 Modeling of elastic deformation of multilayers due to residual stresses and external bending *J. Appl. Phys.* **91** 9652–6
[20] Hsueh C H 2002 Thermal stresses in elastic multilayer systems *Thin Solid Film* **418** 182–8
[21] Wei S, Li B, Fujimoto T and Kojima I 1998 Surface morphological modification of Pt thin films induced by growth temperature *Phys. Rev.* B **58** 3605–8
[22] Kingon A I 1991 Thin films for microelectronics *Ceramic Materials for Electronics* ed R C Buchanan (New York: Dekker) p 485
[23] Hsueh C H, Luttrell C R, Lee S, Wu T C and Lin H Y 2006 Interfacial peeling moments and shear forces at free edges of multilayers subjected to thermal stresses *J. Am. Ceram. Soc.* **89** 1632–8